Published in final edited form as:
*Int J Gynecol Cancer*. 2011 November ; 21(8): 1472–1478. doi:10.1097/IGC.0b013e31822b451d.

# Optimization of Near-Infrared Fluorescent Sentinel Lymph Node Mapping in Cervical Cancer Patients

**Joost R. van der Vorst, M.D.**[1,*], **Merlijn Hutteman, M.Sc.**[1,*], **Katja N. Gaarenstroom, M.D. Ph.D.**[2], **Alexander A.W. Peters, M.D. Ph.D.**[2], **J. Sven D. Mieog, M.D.**[1], **Boudewijn E. Schaafsma, M.D.**[1], **Peter J.K. Kuppen, Ph.D.**[1], **John V. Frangioni, M.D., Ph.D.**[3,4], **Cornelis J.H. van de Velde, M.D., Ph.D.**[1], and **Alexander L. Vahrmeijer, M.D., Ph.D.**[1]

[1]Department of Surgery, Leiden University Medical Center, Leiden, The Netherlands [2]Department of Gynecology and Obstetrics, Leiden University Medical Center, Leiden, The Netherlands [3]Department of Radiology, Beth Israel Deaconess Medical Center, Boston, MA 02215 [4]Division of Hematology/Oncology, Department of Medicine, Beth Israel Deaconess Medical Center, Boston, MA 02215

## Abstract

**Objective—**In early cervical cancer, a total pelvic lymphadenectomy is the standard of care even though most patients have negative nodes and thus undergo lymphadenectomy unnecessarily. Although the value of sentinel lymph node mapping in early stage cervical cancer has not yet been established, near-infrared (NIR) fluorescence imaging is a promising technique to perform this procedure. NIR fluorescence imaging is based on invisible NIR light and can provide high sensitivity, high-resolution, and real-time image-guidance during surgery.

**Methods/materials—**Clinical trial subjects were 9 consecutive cervical cancer patients undergoing total pelvic lymphadenectomy. Prior to surgery, 1.6 mL of indocyanine green adsorbed to human serum albumin (ICG:HSA) was injected transvaginally and submucosally in 4 quadrants around the tumor. Patients were allocated to 500, 750, or 1,000 μM ICG:HSA concentration groups. The Mini-FLARE™ imaging system was used for NIR fluorescence detection and quantitation.

**Results—**Sentinel lymph nodes were identified in all 9 patients. An average of 3.4 ± 1.2 sentinel lymph nodes was identified per patient. No differences in signal to background of the sentinel lymph nodes between the 500, 750, and 1,000 μM dose groups were found ($P = 0.73$). In 2

Corresponding author: Dr. Alexander L. Vahrmeijer, M.D., Ph.D., Albinusdreef 2, 2300 RC Leiden, Phone: +31715262309, Fax: +31715266750, a.l.vahrmeijer@lumc.nl.
*Both authors contributed equally to the study and share first authorship.

**CONFLICT OF INTEREST STATEMENT** Joost R. van der Vorst, M.D.: None.
Merlijn Hutteman, M.Sc.: None.
Katja N. Gaarenstroom, M.D., Ph.D.: None
Alexander A.W. Peters, M.D., Ph.D.: None
J. Sven D. Mieog, M.D.: None.
Boudewijn. E. Schaafsma,, M.D.: None
Peter J.K. Kuppen, Ph.D.: None
John V. Frangioni, M.D., Ph.D.: Mini-FLARE™ technology is owned by Beth Israel Deaconess Medical Center, a teaching hospital of Harvard Medical School. As inventor, Dr. Frangioni may someday receive royalties if products are commercialized. Dr. Frangioni is the founder and unpaid director of The FLARE Foundation, a non-profit organization focused on promoting the dissemination of medical imaging technology for research and clinical use.
Cornelis J.H. van de Velde, M.D., Ph.D.: None.
Alexander L. Vahrmeijer, M.D., Ph.D.: None.

patients, tumor-positive lymph nodes were found. In both patients, tumor-positive lymph nodes confirmed by pathology were also NIR fluorescent.

**Conclusions—**This study demonstrated preliminary feasibility to successfully detect sentinel lymph nodes in cervical cancer patients using ICG:HSA and the Mini-FLARE™ imaging system. When considering safety, cost-effectiveness, and pharmacy preferences, an ICG:HSA concentration of 500 μM was optimal for sentinel lymph node mapping in cervical cancer patients.

### Keywords

Near-Infrared Fluorescence Imaging; Image-Guided Surgery; Cervical Cancer; Sentinel Lymph Node Mapping; Indocyanine Green

## INTRODUCTION

Approximately 11,000 women are diagnosed with cervical cancer annually in the United States, resulting in over 4,000 deaths per year (1). Cervical cancer is also the most common cause of cancer-related death in women in developing countries (2). The prognosis of cervical cancer patients depends on tumor stage and tumor size, but nodal status remains the single most important prognostic factor. The surgical treatment of invasive cervical cancer depends upon the FIGO stage of the patient at time of diagnosis (3). In early stage cervical cancer, a radical hysterectomy is performed in combination with a bilateral pelvic lymphadenectomy to detect lymphatic spread. Nodal tumor involvement occurs in up to 27% of early stage cervical cancer patients (4) and in these patients, radiotherapy or chemoradiation is the primary treatment of choice (5). Therefore, a total lymphadenectomy is performed unnecessarily in a substantial fraction of patients, exposing them to the risk of lymphedema and surgical injuries.

SLN mapping and biopsy is an accepted procedure for vulvar cancer, cutaneous melanomas, and breast cancer; however, its reliability for clinical use in the treatment of early stage cervical cancer has not yet been established (6;7). Research on the use of the SLN procedure in early stage cervical cancer patients has been extensively described using a blue dye, a radiocolloid such as $^{99m}$Technetium ($^{99m}$Tc), or a combination of both with various results (8;9). Van de Lande et al. published a literature review involving over 800 patients with cervical cancer in which they described detection rates of 84%, 88%, and 97% when using blue dye alone, $^{99m}$Tc alone, or a combination of both, respectively (10). Regarding the sensitivity to detect the SLNs, $^{99m}$Tc, alone or in combination with blue dye, yielded the highest pooled sensitivity (92%, range 79%-98%); however, this was not significantly higher than the pooled sensitivity of blue dye alone (82%, range 67%-92%).

Due to the midline position of the cervix, it often has a bilateral multifarious drainage pattern, which makes the SLN procedure in cervical cancer patients more challenging than in breast cancer patients, for example. The main lymphatic drainage patterns have been described previously (11), and several studies have shown that satisfactory SLN detection in cervical cancer is established when SLNs are detected on both sides of the pelvis. Of note, status of a SLN on one side of the pelvis does not predict the nodal status of the other side (12).

NIR fluorescence imaging is a technique that can be used in real time during surgery. This technique uses invisible near-infrared light that can be visualized using specialized camera systems (13). NIR fluorescence imaging has several advantages, such as relatively high tissue penetration (up to 5 millimeters without special techniques), low autofluorescence, and the lack of ionizing radiation (14). Recent preclinical and clinical studies have demonstrated that near-infrared (NIR) fluorescence imaging using the NIR fluorescence

agent indocyanine green (ICG) enables real-time intraoperative visualization of lymphatic channels and detection of the SLNs in various forms of cancer without the need for radioactivity (15). Furthermore, previous preclinical work has demonstrated that adsorption of ICG to human serum albumin (HSA, complex is ICG:HSA) increases the fluorescence intensity and the hydrodynamic diameter, thereby providing improved detection and better retention in the SLN (16).

Crane et al. recently described that the use of NIR fluorescence imaging in cervical cancer patients is technically feasible (17). ICG was injected after laparotomy. In this pilot study, a detection rate of 60% was reached, bilateral SLNs were detected in 30% of patients and 1 of 2 patients who had nodal involvement was false-negative.

The aim of the current study was to assess the intraoperative use of NIR fluorescence imaging using ICG:HSA and the Mini-FLARE™ imaging system in SLN biopsy in cervical cancer patients. A secondary goal was to optimize the dose of the ICG:HSA NIR fluorescent lymphatic tracer.

## MATERIALS AND METHODS

### Preparation of Indocyanine Green Adsorbed to Human Serum Albumin

ICG (25 mg vials) was purchased from Pulsion Medical Systems (Munich, Germany) and was resuspended in 10 cc of sterile water for injection to yield a 2.5-mg/ml (3.2 mM) stock solution for the 500-μM concentration group. Of this solution, 7.8 cc was transferred to a 50-cc vial of Cealb (20% human serum albumin (HSA) solution; Sanquin, Amsterdam, The Netherlands) to yield ICG in HSA (ICG:HSA) at a final concentration of 500 μM. ICG (25 mg vials) was resuspended in 5 cc of sterile water for injection to yield a 5.0 mg/ml (6.4 mM) for the 750-μM and 1,000-μM concentration groups. Of this solution, 5.8 cc or 7.8 cc was transferred to a 50-cc vial of Cealb (20% human serum albumin (HSA) solution to yield ICG in HSA (ICG:HSA) at a final concentration of 750 μM or 1,000 μM, respectively.

### Intraoperative NIR Imaging System (Mini-FLARE™)

SLN mapping was performed using the Mini-FLARE™ image-guided surgery system as described by Mieog et al. (15). Briefly, the system consists of 2 wavelength-isolated light sources: a “white” light source, generating 26,600 lx of 400-650 nm light and a “near-infrared” light source, generating 7.7 mW/cm$^2$ of 760 nm light. Color video and NIR fluorescence images are simultaneously acquired and displayed in real time using custom optics and software that separate the color video and NIR fluorescence images. A pseudo-colored (lime green) merged image of the color video and NIR fluorescence images is also displayed. The imaging head is attached to a flexible gooseneck arm, which permits positioning of the imaging head virtually anywhere over the surgical field, and at extreme angles. For intraoperative use, the imaging head and imaging system pole stand are wrapped in a sterile shield and drape (Medical Technique Inc., Tucson, AZ).

### Clinical Trial

The single-institution clinical trial was approved by the Medical Ethics Committee of the Leiden University Medical Center and was performed in accordance with the ethical standards of the Helsinki Declaration of 1975. A total of 9 consecutive patients with cervical cancer that planned to undergo a radical abdominal trachelectomy or a radical hysterectomy and a total pelvic lymphadenectomy were included. All patients provided informed consent and were anonymized. Exclusion criteria were pregnancy, lactation or an allergy to iodine, shellfish, or indocyanine green. All procedures were performed by 2 gynecologists who were assisted by experienced researchers. Before the start of surgery, 1.6 mL ICG:HSA

(concentration: 500, 750 or 1,000 μM) was transvaginally injected submucosally in 4 quadrants around the cervical tumor using a 21G, 1½ inch needle. Directly after the ICG:HSA injection, surgical scrub and sterile covering of the operation field commenced, and a laparotomy was performed. Before the systematic pelvic lymphadenectomy was performed, all standard locations (along the external iliac vessels and the hypogastric artery, along the common iliac artery, the obturator fossa and the lateral parametrium) were examined for NIR fluorescence using the Mini-FLARE™ imaging system. Fluorescent hotspots exhibiting a signal-to-background ratio (SBR) ≥ 1.1 *in vivo* were considered positive by NIR fluorescence. All fluorescent hotspots were denominated as SLNs and were subsequently resected and measured for fluorescence *ex vivo*. Then, the systemic pelvic lymphadenectomy was performed and all resected LNs were also measured for fluorescence *ex vivo*. Lymphadenectomy consisted of removal of all lymph node-bearing fatty tissue along the external iliac vessels, the common iliac artery, the hypogastric artery, and from the obturator fossa (18). Also, the area lateral to and underneath the superior vesical arteries (lateral parametrium) was cleared from the lymphatic tissue. The radical hysterectomy and abdominal trachelectomy were performed according to the standard procedure. In case of a radical trachelectomy, histopathological frozen analysis was performed and when nodes were found to contain metastases, a hysterectomy was performed in addition. Afterwards, all resected lymph nodes were examined by routine histopathological analysis, and lymph nodes were fixed in formalin and embedded in paraffin for routine hematoxylin and eosin staining. SLNs and non-SLNs were examined separately.

### Statistical Analysis

For statistical analysis and to generate graphs, GraphPad Prism Software (Version 5.01, La Jolla, CA) was used. Differences in SBR between concentration groups were tested with a one-way analysis of variance (ANOVA) with subsequent pairwise comparisons corrected according to the Bonferroni correction. Assumption of equal variances was confirmed using Levene's test. All statistical tests were two-tailed and $P < 0.05$ was considered significant.

## RESULTS

### Patient and Tumor Characteristics

Patient and tumor characteristics are described in Table 1. Nine patients with stage Ib cervical cancer undergoing primary surgery were included in the study. Of these patients, median BMI was 21 (range 18-35), median age was 40 years (range 29-77 years), and median tumor size was 3.05 cm (range 0.7-11 cm). One patient presented with an exophytic cervical tumor measuring 11 cm in length and 4 cm in width protruding into the vagina. Five patients underwent a radical hysterectomy and 3 patients underwent a radical trachelectomy. In one patient, extensive endometriosis precluded radical hysterectomy. In this patient, the uterus was left in situ, but a pelvic lymphadenectomy was performed.

### Intraoperative NIR Fluorescence Imaging

In all patients (N = 9), NIR fluorescence imaging enabled identification of 1 or more fluorescent hotspots. An example of the NIR fluorescence images of the procedure in cervical cancer is shown in Figure 1. Average time between injection of ICG:HSA and NIR fluorescence imaging was 51 ± 18 min. A total of 31 fluorescent hotspots were detected. On average, 3.4 ± 1.2 (range 1-5) fluorescent hotspots per patient were identified by NIR fluorescence (Table 2). Within these hotspots, a total of 41 lymph nodes were found after histopathological examination, yielding an average of 4.6 ± 2.1 true lymph nodes per patient . In 3 fluorescent hotspots, adipose tissue only, with no lymph tissue present, was found after histopathological examination. An average of 25.1 lymph nodes (range 10-39)

per patient were harvested. Histological analysis showed that 2 of 9 patients had metastases in a total of 3 SLNs. No other lymph node metastases were observed.

### Localization of Sentinel Lymph Nodes

A total of 31 fluorescent hotspots were confirmed to be SLNs. All SLNs were pelvic nodes and were identified along the left (n = 8) and right (n = 6) external iliac vessels, the right common iliac vessels (n = 4), the left (n = 5) and right (n = 4) obturator fossa, and the left (n = 2) and right (n = 2) lateral parametrium. Table 2 provides exact locations for all SLNs. In 8 of 9 patients, bilateral SLNs were found. After histological confirmation, 3 positive SLNs were found in 2 patients. In the first patient, the positive SLNs were located in the left lateral parametrium and along the right external iliac vessels. In the second patient, the positive SLN was located along the left external iliac vessels.

### *Ex vivo* imaging of lymph nodes

All lymph nodes were examined for fluorescence *ex vivo* using the Mini-FLARE™ imaging system. In 4 of 9 patients additional fluorescent hotspots (N=10) were identified, which were not identified during *in vivo* NIR fluorescence imaging (Table 2). Within 8 of these 10 hotspots, a total of 10 lymph nodes were found after histopathological examination and within 2 of 10 these hotspots, adipose tissue only, with no lymph node tissue present, was found after histopathological examination. The hotspots that contained lymph nodes were harvested along the left (n = 1) and the right (n = 1) external iliac vessels, and the left (n = 1) and the right (n = 5) obturator fossa. The hotspots that contained only adipose tissue were harvested along the left (n = 1) and the right (n = 1) external iliac vessels. No additional metastases were found during *ex vivo* analysis.

### Optimization of ICG:HSA Dose

In all dose groups (500, 750, and 1,000 μM), fluorescence intensity of the SLN was significantly higher than the fluorescence intensity of surrounding tissue ($P<0.001$). Mean SBRs of the SLNs were 10.1 ± 1.2, 10.3 ± 1.2 and 12.0 ± 5.7 for the 500 μM, 750 μM, and 1,000 μM dose groups, respectively (Figure 2). A one-way ANOVA test showed no significant differences in SBRs of SLNs between the different dose groups ($P = 0.76$).

## DISCUSSION

The current study showed the feasibility of the SLN procedure in early stage cervical cancer patients using ICG:HSA and the Mini-FLARE™ imaging system. The Mini-FLARE™ imaging system that was used in the current study displays NIR fluorescence signal, color signal, and a merge of both and illuminates the surgical field with white light. This enabled the gynecologist to perform the SLN detection and resection under direct image guidance. The imaging head of the Mini-FLARE™ system is attached to a flexible gooseneck arm, which permitted flexible positioning of the imaging head at extreme angles over the surgical field. This is of particular importance in large abdominal surgery. During all procedures, intraoperative imaging using this imaging system was successful and uneventful.

No differences in SBR of the SLNs between the 500, 750, and 1,000 μM dose groups were found. The location of the NIR fluorescent SLNs was in concordance with formerly published drainage patterns (11). Furthermore, bilateral SLNs were found in 8 of 9 patients. The 3 tumor-positive SLNs (in 2 patients) were located along the left external iliac vessels (n = 1), the right external iliac vessels (n = 1), and in the left lateral parametrium (n = 1). Identification of a parametrial SLN is rather remarkable because there is presently no consensus on removal of parametrial lymph nodes during total pelvic lymphadenectomy (19-22). Although larger clinical trials will be required to answer this question, from this

study we can at least conclude that parametrial lymph nodes are identifiable using ICG:HSA and Mini-FLARE™.

The detection rate of SLNs in our pilot-study was 100% and this detection rate is in concordance with a prospective, multicenter cohort study of 590 patients that examined SLN mapping in cervical cancer patients and observed a detection rate of 93.5% when a combination of patent blue and radiocolloids was used (23). In the current study, on average, a total of 3.4 SLNs were identified per patient intraoperatively, which is also consistent with previously published data (8;9). In the recently published study by Crane et al. (17) on NIR fluorescence SLN mapping in cervical cancer patients, ICG was injected after laparotomy and NIR fluorescence measurements were made directly after injection. Furthermore, ICG was diluted in patent blue prior to injection. These differences in study design along with the use of a different imaging system hinder a direct comparison of the results.

The optimal time interval between injection of ICG:HSA and NIR fluorescence imaging is still unknown. Nevertheless, timing of imaging could be of great importance in terms of detection rate, sensitivity, and SBRs of SLNs. The mean interval between administration of ICG:HSA and NIR fluorescence measurements in the current study was 51 min. This time interval was relatively long because the ICG:HSA injection was performed prior to surgery, followed by surgical scrub and operation time to expose the iliac vessels. During surgery, no more than several minutes were needed for SLN detection and resection.

*Ex vivo* NIR fluorescence imaging of total lymphadenectomy specimens detected 10 additional fluorescent hotspots in 4 of 9 patients. Detection of these additional fluorescent hotspots during *ex vivo* imaging could possibly be explained by the relatively long time interval between ICG:HSA administration and performance of the total lymphadenectomy. Although ICG:HSA has an improved hydrodynamic diameter compared to ICG alone, passage through the SLN to second tier nodes can still possibly occur if the time interval is long enough. An alternative explanation for the additional *ex vivo* detected fluorescent hotspots is that these hotspots were missed *in vivo* due to technical limitations, as for example, the limited penetration depth (millimeters) for NIR fluorescent light. Future larger studies are needed to optimize timing and to evaluate the importance of additional fluorescent hotspots that are missed *in vivo* and are detected in the resection specimen. Nevertheless, to bypass this pitfall, the development of new lymphatic tracers that are retained in the SLN without flowing through to higher tier nodes is imperative to optimize NIR fluorescence SLN mapping in cervical cancer.

In the current study, fluorescent hotspots were found *in vivo* (n = 3) and *ex vivo* (n = 2) that did not contain lymphatic tissue but consisted of adipose tissue, which is not an uncommon observation in the SLN procedure. A plausible explanation for these fluorescent hotspots is that fluorescent lymph fluid can exit the lymphatic channel, due to extensive manipulation during surgery or anatomical aberrations, for example. If detection of a relatively small number of these hotspots does not obfuscate the identification of the true SLNs, this phenomenon does not negatively influence the SLN procedure.

In a recently published dose-finding clinical study performed by our group using NIR fluorescence SLN mapping in breast cancer patients, an optimal ICG:HSA dose range between 400 and 800 μM was found (15). In the 1,000 μM ICG:HSA dose group, the fluorescent intensity and the SBR of the SLNs decreased, most probably caused by an effect known as fluorescence quenching (24). In the current study, no differences were found in SBRs between the 500, 750, and 1,000 μM dose groups. This lack of difference combined with pharmacy preferences, safety, previous results, and costs make a dose of 500 μM most convenient to perform the SLN procedure in cervical cancer patients.

As in other areas of surgery, the use of laparoscopy is expanding in cancer surgery. Lymphadenectomies are being performed laparoscopically as standard of care in several centers. NIR fluorescence may also be of great value in laparoscopic surgery because palpation is not possible and the surgeon can only rely on visual inspection and preoperative imaging. To implement NIR fluorescence in laparoscopic surgery, laparoscopic NIR fluorescence camera systems are currently being developed and tested (25).

In conclusion, we assessed the potential value of NIR fluorescence imaging in SLN mapping in early stage cervical cancer patients. Although sample size was small, this study showed a high SLN detection rate (100%) and no false-negative lymph nodes. However, to prove actual patient benefit and to assess sensitivity more precisely, larger clinical trials will be necessary.

## Acknowledgments

The authors thank Margriet J.G. Löwik and Dorien M.A. Berends-van der Meer for their assistance during the patient inclusion process and Lindsey Gendall for editing. This work was supported in part by the Nuts Ohra Fund, the Foundation “Maurits and Anna de Kock,” and National Institutes of Health grant R01-CA-115296. This work was supported by a Royal Dutch Academy of Arts and Sciences visiting professorship granted to John V. Frangioni.

## References

1. Jemal A, Siegel R, Ward E, et al. Cancer statistics, 2009. CA Cancer J Clin. 2009 Jul; 59(4):225–49. [PubMed: 19474385]
2. Ferlay, J.; Bray, F.; Pisani, P.; Parkin, D. GLOBOCAN: Cancer Incidence, Mortality and Prevalence Worldwide. 1. Lyon: IARCPress; 2001.
3. Hacker NF. Revised FIGO staging for carcinoma of the vulva. Int J Gynaecol Obstet. 2009 May; 105(2):105–6. [PubMed: 19329116]
4. Horn LC, Hentschel B, Fischer U, et al. Detection of micrometastases in pelvic lymph nodes in patients with carcinoma of the cervix uteri using step sectioning: Frequency, topographic distribution and prognostic impact. Gynecol Oncol. 2008 Nov; 111(2):276–81. [PubMed: 18722005]
5. Green J, Kirwan J, Tierney J, et al. Concomitant chemotherapy and radiation therapy for cancer of the uterine cervix. Cochrane Database Syst Rev. 2005; (3):CD002225. [PubMed: 16034873]
6. Van Der Zee AG, Oonk MH, De Hullu JA, et al. Sentinel node dissection is safe in the treatment of early-stage vulvar cancer. J Clin Oncol. 2008 Feb 20; 26(6):884–9. [PubMed: 18281661]
7. Morton DL, Wen DR, Wong JH, et al. Technical details of intraoperative lymphatic mapping for early stage melanoma. Arch Surg. 1992 Apr; 127(4):392–9. [PubMed: 1558490]
8. Levenback C, Coleman RL, Burke TW, et al. Lymphatic mapping and sentinel node identification in patients with cervix cancer undergoing radical hysterectomy and pelvic lymphadenectomy. J Clin Oncol. 2002 Feb 1; 20(3):688–93. [PubMed: 11821449]
9. Marchiole P, Buenerd A, Scoazec JY, et al. Sentinel lymph node biopsy is not accurate in predicting lymph node status for patients with cervical carcinoma. Cancer. 2004 May 15; 100(10):2154–9. [PubMed: 15139058]
10. van de Lande J, Torrenga B, Raijmakers PG, et al. Sentinel lymph node detection in early stage uterine cervix carcinoma: a systematic review. Gynecol Oncol. 2007 Sep; 106(3):604–13. [PubMed: 17628644]
11. Ercoli A, Delmas V, Iannone V, et al. The lymphatic drainage of the uterine cervix in adult fresh cadavers: anatomy and surgical implications. Eur J Surg Oncol. 2010 Mar; 36(3):298–303. [PubMed: 19628364]
12. Silva LB, Silva-Filho AL, Traiman P, et al. Sentinel node detection in cervical cancer with (99m)Tc-phytate. Gynecol Oncol. 2005 May; 97(2):588–95. [PubMed: 15863164]
13. Vahrmeijer AL, Frangioni JV. Seeing the invisible during surgery. Br J Surg. 2011 Jun; 98(6):749–50. [PubMed: 21484776]

14. Frangioni JV. In vivo near-infrared fluorescence imaging. Curr Opin Chem Biol. 2003 Oct; 7(5): 626–34. [PubMed: 14580568]
15. Mieog JS, Troyan SL, Hutteman M, et al. Towards Optimization of Imaging System and Lymphatic Tracer for Near-Infrared Fluorescent Sentinel Lymph Node Mapping in Breast Cancer. Ann Surg Oncol. 2011 in press.
16. Ohnishi S, Lomnes SJ, Laurence RG, et al. Organic alternatives to quantum dots for intraoperative near-infrared fluorescent sentinel lymph node mapping. Mol Imaging. 2005 Jul; 4(3):172–81. [PubMed: 16194449]
17. Crane LM, Themelis G, Pleijhuis RG, et al. Intraoperative Multispectral Fluorescence Imaging for the Detection of the Sentinel Lymph Node in Cervical Cancer: A Novel Concept. Mol Imaging Biol. 2010 Sep 11.
18. Pieterse QD, Kenter GG, Gaarenstroom KN, et al. The number of pelvic lymph nodes in the quality control and prognosis of radical hysterectomy for the treatment of cervical cancer. Eur J Surg Oncol. 2007 Mar; 33(2):216–21. [PubMed: 17097845]
19. Bader AA, Winter R, Haas J, et al. Where to look for the sentinel lymph node in cervical cancer. Am J Obstet Gynecol. 2007 Dec; 197(6):678–7. [PubMed: 18060980]
20. Steed H, Capstick V, Schepansky A, et al. Early cervical cancer and parametrial involvement: is it significant? Gynecol Oncol. 2006 Oct; 103(1):53–7. [PubMed: 16516279]
21. Winter R, Haas J, Reich O, et al. Parametrial spread of cervical cancer in patients with negative pelvic lymph nodes. Gynecol Oncol. 2002 Feb; 84(2):252–7. [PubMed: 11812083]
22. Photopulos GJ, Zwaag RV. Class II radical hysterectomy shows less morbidity and good treatment efficacy compared to class III. Gynecol Oncol. 1991 Jan; 40(1):21–4. [PubMed: 1989910]
23. Altgassen C, Hertel H, Brandstadt A, et al. Multicenter validation study of the sentinel lymph node concept in cervical cancer: AGO Study Group. J Clin Oncol. 2008 Jun 20; 26(18):2943–51. [PubMed: 18565880]
24. Gioux S, Choi HS, Frangioni JV. Image-guided surgery using invisible near-infrared light: fundamentals of clinical translation. Mol Imaging. 2010 Oct; 9(5):237–55. [PubMed: 20868625]
25. van der Poel HG, Buckle T, Brouwer OR, et al. Intraoperative Laparoscopic Fluorescence Guidance to the Sentinel Lymph Node in Prostate Cancer Patients: Clinical Proof of Concept of an Integrated Functional Imaging Approach Using a Multimodal Tracer. Eur Urol. 2011 Mar 30.

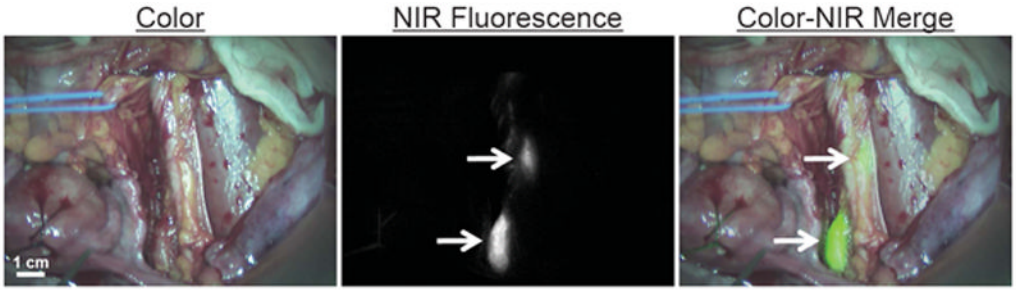


**Figure 1.**
Near-infrared fluorescence-based SLN mapping using ICG:HSA and Mini-FLARE. Identification of 2 SLNs (arrows), located along the left iliac vessels, with NIR fluorescence imaging is demonstrated in a cervical cancer patient, 45 minutes after administration of 750 μM ICG:HSA. Camera exposure time was 100 milliseconds. Scale bar represents 1 cm.

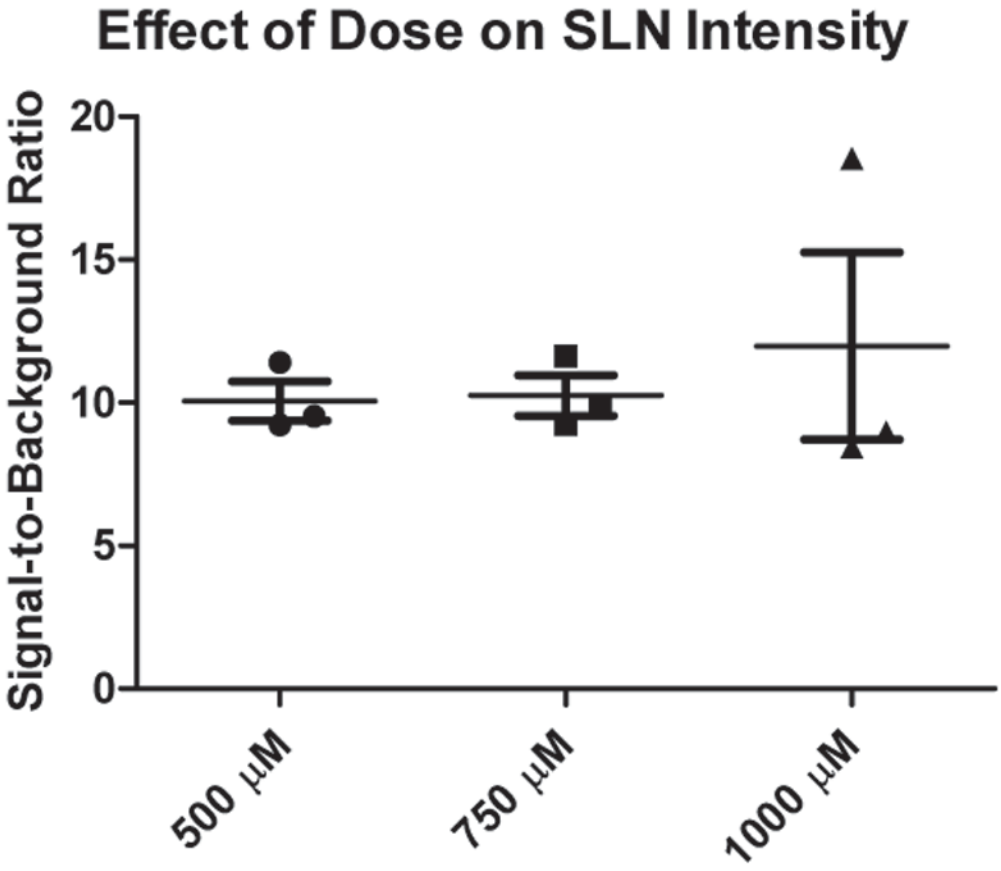


**Figure 2.**
Brightness of SLNs as a function of ICG:HSA dose. Signal-to-background ratio (mean ± SD) of the SLNs (ordinate) as a function of injected dose of ICG:HSA (abscissa). Statistical comparisons are as follows: the SBRs of the 500-, 750-, and 1000- μM concentration groups were not significantly different.

**Table 1**

Patient and Tumor Characteristics

| Patient no. | ICG:HSA Dose (μM) | Age (Years) | BMI | FIGO Stage | Type of Surgery | Tumor Type | Tumor Size (cm) |
|---|---|---|---|---|---|---|---|
| 1 | 500 | 35 | 35 | IB1 | Radical Trachelectomy | Adenosquamous | 2.5 |
| 2 | 500 | 43 | 26 | IB2 | Radical Hysterectomy | Squamous | 4.5 |
| 3 | 500 | 77 | 21 | IB2 | Radical Hysterectomy | Squamous | 11.0 |
| 4 | 750 | 46 | 30 | IB1 | No resection | Squamous | n/a |
| 5 | 750 | 59 | 21 | IB1 | Radical Hysterectomy | Squamous | 4.2 |
| 6 | 750 | 29 | 22 | IB1 | Radical Trachelectomy | Squamous | 2.5 |
| 7 | 1000 | 30 | 18 | IB1 | Radical Trachelectomy | Squamous | 1.0 |
| 8 | 1000 | 40 | 20 | IB1 | Radical Hysterectomy | Squamous | 0.7 |
| 9 | 1000 | 34 | 21 | IB1 | Radical Hysterectomy | Squamous | 3.6 |

**Table 2**

Results from *In Vivo* and *Ex Vivo* SLN Imaging

| Patient no. | NIR Hotspots *In Vivo* | Additional NIR Hotspots *Ex Vivo* | Total LNs Harvested | Tumor-Positive SLNs From Pathology | Tumor-Positive SLNs that were NIR Fluorescent | False-Negatives | Location of NIR Fluorescent SLNs | Injection-Imaging Interval (min) | Bilateral SLNs Identified |
|---|---|---|---|---|---|---|---|---|---|
| 1 | 3 | 3 | 15 | 0 | 0 | n/a | Left (1) and right (1) external iliac, left obturator (1) | 94 | Yes |
| 2 | 4 | 0 | 36 | 2 | 2 | 0 | Left (1) and right (1) parametrium, right external iliac (1), right common iliac (1) | 35 | Yes |
| 3 | 3 | 0 | 17 | 0 | 0 | n/a | Left external iliac (1) left obturator (2) | 43 | Yes |
| 4 | 3 | 1 | 23 | 0 | 0 | n/a | Left (1) and right (1) external iliac, left obturator (1) | 44 | Yes |
| 5 | 4 | 0 | 39 | 0 | 0 | n/a | Left (1) and right (1) external iliac, right parametrium (1), right common iliac (1) | 40 | Yes |
| 6 | 5 | 0 | 33 | 0 | 0 | n/a | Left (1) and right (1) external iliac, right common iliac (1), left obturator (1), left parametrium (1) | 44 | Yes |
| 7 | 1 | 0 | 16 | 0 | 0 | n/a | Right obturator (1) | 41 | No |
| 8 | 5 | 2 | 37 | 0 | 0 | n/a | Left (1) and right (1) external iliac, right common iliac (1) obturator right (2) | 62 | Yes |
| 9 | 3 | 4 | 10 | 1 | 1 | 0 | Left (2) and right (1) external iliac | 58 | Yes |
| | 31 | 10 | 226 | 3 | 3 | 0 | | Average = 51 ± 18 | |